**Layer-by-Layer Assembly of Nacre-Like Nanostructured Composites with Antimicrobial Properties**

*Paul Podsiadlo[#§], Stephen Paternel[#§], Jean-Marie Rouillard[#], Zhengfei Zhang[†], Jaebeom Lee[#], Jung-Woo Lee[#], Erdogan Gulari[#], Nicholas A. Kotov[#*]*

*[#] Department of Chemical Engineering, The University of Michigan, Ann Arbor, Michigan, 48109, USA*
*[†] Department of Mechanical Engineering, The University of Michigan, Ann Arbor, Michigan, 48109, USA*
** To whom correspondence should be addressed: Tel.: (734) 763-8768, Fax: (734) 764-7453, E-mail: kotov@umich.edu*
*[§] Contributed Equally*

## ABSTRACT

In a recent report, we have presented layer-by-layer (LBL) assembly of a biomimetic nanostructured composite from montmorillonite clay nanosheets and poly(diallylmethyl ammonium chloride) (*Nature Materials,* 2003, 2, 413). The structure, deformation mechanism, and mechanical properties of the material are very similar to those of natural nacre and lamellar bones. This fact prompts further investigation of these composites as potential bone implants. LBL assembly affords preparation of multifunctional composites and here we demonstrate that not only mechanical strength, but also antibacterial activity can be introduced in these implantable materials by alternating clay layers with starch-stabilized silver nanoparticles. The resulting composite showed excellent structural stability with no detectable levels of silver lost over one month period. Evaluation of antibacterial properties showed almost complete growth inhibition of *E. coli* over an 18 hours period. The amount of silver eluted from the LBL composite over one month period was determined to be only 0.5-3.0 μg/L. This concentration of silver did not prevent the growth of the mammalian tissue cultures. The LBL composite has shown biocompatibility with human osteoblast cell line.

## INTRODUCTION

Integrating the properties of organic and inorganic composites in thin films has recently been a subject of intense study. The layer-by-layer (LBL) assembly technique, based on sequential adsorption of a substrate in solutions of oppositely charged compounds, continues to be one of the most popular and well-established methods for formation of multilayer thin films. While first performed with polyelectrolytes in the early 1990s by Decher et al.[1], LBL assembly has since expanded to include compounds such as nanoparticles (NPs), clays, and organic matter such as proteins. The wide variety of species has led to a number of potential research and industrial applications in semiconductors[2,3], catalysts[4,5], optics[6-8], magnetic devices[9,10], and sensors[11,12]. LBL assembly has gained its popularity in part due to its relative simplicity, requiring a minimum of setup and expensive equipment. Film thickness is typically of nanometer scale, and deposition can be precisely controlled by adjusting process conditions such as solution pH, ionic strength, and immersion time. Recent work has also demonstrated patterned deposition control through polymer-on-polymer stamping[13]. Unlike spin-coating, LBL assembly can produce homogeneous films with little or no phase separation[14], and can also be used to build films on substrates with complex geometries[15].

LBL assembly has also proven invaluable in its ability to merge the functionalities of its components. Through creative experimental setup, one can combine the physical properties of NPs and proteins with the mechanical properties of clays and polymers. The addition of collagen to CdTe NP assemblies, for example, has been found to increase biocompatibility[16], and monolayers of montmorillonite clay have also been found to control interactions between layers of gold NPs[17]. Combined assemblies of montmorillonite clay and magnetite NPs have led to free-standing NPs films[18]. In fact, our group has found that sufficient number of layers of the polyelectrolyte poly(diallyldimethylammonium chloride) (PDDA) and montmorillonite can lead to a free-standing film with mechanical properties similar to those of nacre and lamellar bone[19]. As demonstrated by the group of V. Tsukruk, incorporation of Au NPs in the polyectrolyte films also resulted in free-standing films with excellent mechanical properties and unique potential applications[20, 21].

Such assemblies are recently gaining popularity in the field of biomaterials, creating a demand for biocompatible and antimicrobial thin films as potential coatings for biomedical implants. A variety of solutions have since been developed using LBL assembly to help meet this demand. Several groups have demonstrated the ability of multilayer films to control adhesion of mammalian cells.[22-26]. Bhadra et al. have shown preparation of hollow multilayer capsules loaded with Ciprofloxacin hydrochloride for sustained delivery of this antimicrobial drug.[27] Boulmedais et al. and Kenausis et al. have both presented preparation of multilayer thin films with anti-adhesive properties for both proteins and bacteria.[28,29] Etienne et al. have prepared an active multilayer coating by incorporation of an antimicrobial peptide into the deposition sequence.[30] LBL assembly by the group of M. Bruening of polyethyleneimine-silver ion complex with a polyanion and subsequent reduction to produce *in-situ* silver NPs[31] as well as dendrimeric[32,33] silver NPs have also been successfully implemented as antimicrobial coatings to combat *E. coli*. Such biocompatible assemblies, however, have yet to be applied to a film with the free-standing mechanical properties of artificial nacre.

This study presents an antimicrobial coating for such structures using a multifunctional LBL assembly of PDDA, montmorillonite, and biocompatible, starch-coated silver NPs prepared using a “green” synthesis strategy. Film homogeneity and deposition were monitored using AFM and UV-vis spectrometry, and film stability was analyzed using ICP-MS. Cell

culture testing was also performed with *E. coli* and mammalian cells to observe bactericidal activity and cytocompatibility. Such antimicrobial coatings could prove effective for a variety of biomedical devices, and help realize the potential bioapplications of these high strength "nacre-like" composites.

## EXPERIMENTAL

### *Materials.*

The polymers poly(diallyldimethylammonium chloride) (PDDA, MW ~100,000 and 200,000) and poly(acrylic acid) (PAA, MW 60,000) were purchased from Sigma-Aldrich (St. Louis, MO) and used as received without further purification. Modified $Na^+$-Montmorillonite, Cloisite $Na^+$ (MTM) was purchased from Southern Clay Products (Gonzales, TX) and used as received. Polymer solutions were diluted to desired concentrations with 18MΩ*$cm^{-1}$, de-ionized water prior to use in the experiments. Starch indicator was a commercial reagent from Fisher Scientific (Hampton, NH). $AgNO_3$ and β-d-glucose, both used in the Ag NPs synthesis, were obtained from Sigma-Aldrich. Microscope glass slides were obtained from Fisher Scientific. Hydrogen peroxide and concentrated sulfuric acid used in the piranha solution were purchased from Sigma-Aldrich. Dulbecco's Modified Eagle Medium (DMEM) was purchased from Fisher Scientific, and fetal bovine serum was purchased from GIBCO (Carlsbad, CA). Ampicillin and human osteoblasts were purchased from American Type Culture Collection (ATCC, Manassas, VA).

### *Silver NP Synthesis.*

Starch-stabilized Ag NPs were synthesized based on a modified "green" synthesis method published previously[34]. Briefly, 200mL of starch indicator was combined with 3.3mL of 0.10M $AgNO_3$ under gentle heating and stirring in the absence of oxygen. Upon dissolution, 5.0mL of 0.10M β-d-glucose reducing agent was added, and the reaction was allowed to proceed for 24 hours. The resulting solution was deep yellow-brown in color, indicating the presence of metallic silver. This mixture was then used as obtained in the layer-by-layer assembly process.

### *Layer-by-layer Assembly of Silver NP Films.*

The microscope glass slides used in LBL assembly were cleaned by immersion in piranha solution (3:1 $H2SO_4$:$H_2O_2$, dangerous if contacted with organics) for 1 hour, then thoroughly rinsed with de-ionized water prior to use. 0.5 wt% MTM dispersion was prepared by dissolving 5g of clay powder in 1000 mL of 18MΩ*$cm^{-1}$ and stirring the solution for 1 week prior to use. In order to achieve greater charge density on the surface, slides were pre-coated with $(PDDA/PAA)_3$ prior to the deposition of PDDA/Ag NPs and PDDA/MTM/PDDA/Ag NPs layers, respectively. In the pre-coating process, the slides were immersed sequentially in 0.5 wt% solution of 100,000 MW PDDA for 10 minutes, rinsed with DI water, and dried under a stream of air, followed by a 10-minute immersion in 1.0 wt% PAA, rinsing, and drying. This sequence was repeated 3 times before continuing with composite deposition.

In a typical sample preparation, a glass slide with a $(PDDA/PAA)_3$ primer layer was immersed in 0.5wt% solution of 200,000 MW PDDA for 10 minutes, rinsed with DI water for 1 minute and dried, then immersed in 0.5 wt% MTM dispersion for 10 minutes, rinsed for 1 minute, and again dried. The procedure was then repeated using PDDA and Ag NPs solution to complete one cycle of (PDDA/MTM/PDDA/Ag NPs). This cycle could then be repeated as necessary to obtain the desired number of layers.

The layer-by-layer assembly process was monitored using an 8453 UV-Vis Chem Station spectrophotometer produced by Agilent Technologies, with data collected after each (PDDA/MTM) and (PDDA/MTM/PDDA/Ag NPs) cycle for up to 10 cycles. Images of (PDDA/MTM) and (PDDA/Ag NPs) layers were obtained using a NanoScope IIIa from Veeco Instruments (Santa Barbara, CA) atomic force microscope operated in tapping mode with silicon nitride cantilever tips.

***Bacterial Inhibition Evaluation.***

Ampicillin-resistant gram-negative bacteria, *E. coli* XL1-Blue strain transformed with the pBluescript II KS(-) plasmid (Statagene, La Jolla, CA) were grown overnight in 50 ml of LB ampicillin (10 g/L tryptone, 10 g/L yeast extract, 5 g/L NaCl, 500 mg/L ampicillin) at 37°C under agitation (350 rpm). An aliquot was used to inoculate a 50 ml flask of fresh LB ampicillin medium. When the culture reached an optical density at 600 nm (OD600) of 0.005 – 0.01 after incubation (37°C, 350 rpm), 1 ml of culture was transferred to a sterile 5ml culture tube (0.5 cm inside diameter test tube, Fisher Scientific) containing a single piece of glass slide 25mm x ~5mm coated using LBL assembly on both sides, and incubated for 18 hours as described above (this is a modified version of the standard shake-flask test, ASTM E2149-01) After incubation, the OD600 was read using UV-Vis spectrophotometer to determine the bacterial growth.

Cell viability of the remaining culture after incubation was assessed by colony forming unit (CFU) counting. Typically, a serial dilution of the culture was plated on LB ampicillin agar plates and incubated overnight at 37°C before counting of the colonies. Fresh colonies in fresh medium were also plated for comparison with the same initial density of cells. After incubation, the viable colonies were visible with naked eye and thus could be counted manually. After counting, the number of colonies was compared with the control plates.

***Biocompatibility Evaluation.***

Human Osteoblast cell (ATCC, CRL-11372) culture was grown until full confluence for 1 week in 13mL of 90% DMEM, 10% FBS, and 1% ampicilin medium at 37 ˚C in humidified incubator with 5% $CO_2$. Square pieces of glass slides (1cm x 1cm): 3x clean without coating, 3x pre-coated only with $(PDDA/PAA)_3$, and 3x coated with $(PDDA/PAA)_3(PDDA/MTM/PDDA/Ag\ NPs)_{10}$ were placed on the bottom of 3 different 12-well plates and sterilized by 70% EtOH immersion followed by 1hour UV irradiation. Cells were then seeded into each well at a density of $\sim 0.1*10^6$ and incubated for three days. Biocompatibility was assessed by observing the attachment and spreading of the cells on the surfaces.

**RESULTS AND DISCUSION**

***Ag NPs Synthesis.***

To avoid potential problems with stabilizer toxicity, the Ag NPs were synthesized following a modified green synthesis protocol, where a macromolecule of biological origin (starch) was used as a stabilizer[34]. Successful synthesis of these starch-stabilized Ag NPs was confirmed with UV-vis absorbance, and the size of resulting NPs was verified with AFM. The UV-vis absorbance spectrum of the deep yellow-brown Ag NPs solution, which was subsequently used in the LBL procedure without modification, is shown in Figure 1. This spectrum shows an absorbance peak at 410 nm, which matches visual observations and is in agreement with the original green synthesis protocol ($\lambda$ = 419 nm). The narrow nature of the observed peak also suggests a uniform mixture of NPs with little variation in particle size,

which otherwise would have resulted in stretching of the Ag NPs absorbance peak. These solutions of NPs were also found to be quite stable, with no evidence of aggregation during two months of storage.

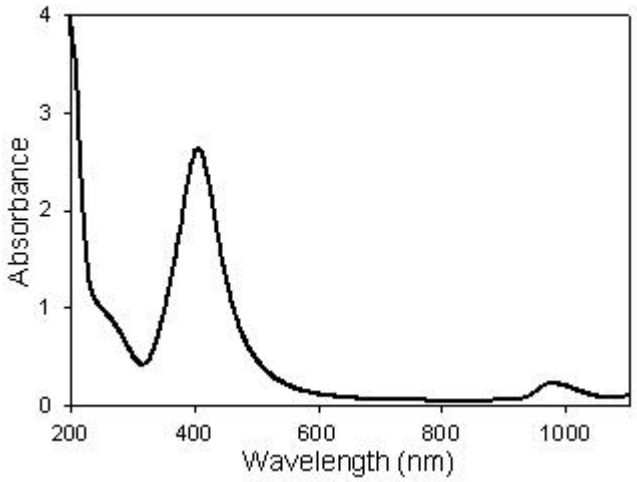


**Figure 1.** UV-vis absorbance spectrum of Ag NPs solution. The maximum absorbance peak occurs at 410nm.

Figure 2A shows the topographic AFM image of a $(PDDA/Ag\ NPs)_1$ bilayer, formed on a silica wafer using 10 minute immersions for each component. The image reveals dense packing of spherical Ag NPs, with AFM cross-sectional analysis (Fig. 2C and 2D) showing an average NP diameter of 4.3 nm ± 1.5 nm (Fig. 2B), which closely correlates with the size reported in the original green synthesis protocol (5.3 nm ± 2.6 nm). This uniform nanoparticle size confirms the lack of variance evidenced by the narrow UV-vis absorbance spectrum in Fig. 1.

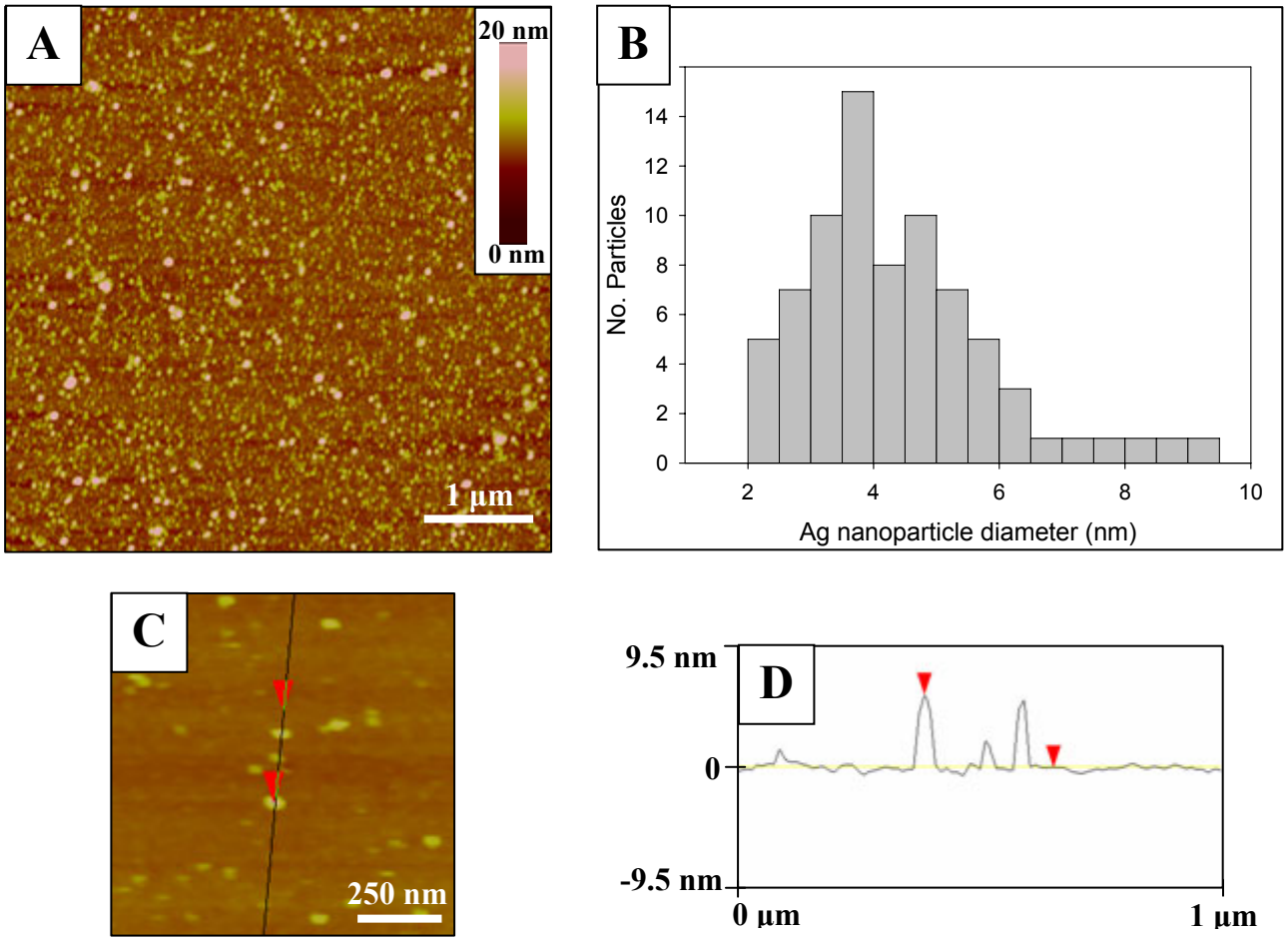


**Figure 2.** AFM characterization of the Ag NPs size distribution: A) topography image of a large area, B) Ag NPs size distribution from counting of 77 particles, C) magnified topography image used for cross-sectional analysis, and D) result of the cross sectional analysis on the particular Ag NPs. Average particle size was found to be 4.3nm ± 1.5 nm.

***Assembly of (PDDA/MTM) Composites.***

To confirm proper LBL assembly of the "artificial nacre" structure (Figure 3A, inset), $(PDDA/MTM)_{10}$ films were assembled on a microscope glass slide using ten-minute immersions for both polymer and clay components. Assembly was monitored with UV-vis absorbance measurements where, as detailed previously[19], successful assembly resulted in linear increase of absorbance with increasing number of layers. Figure 3A is a compilation of UV-vis absorbance spectra collected after deposition of the $(PDDA/PAA)_3$ primer layer and each of the (PDDA/MTM) bilayers. The even increase in absorbance with each additional bilayer suggests regular deposition of PDDA and MTM with each immersion cycle. Successful MTM deposition was also evidenced by the glass slide gradually changing from transparent to opaque (milky color) over the course of deposition.

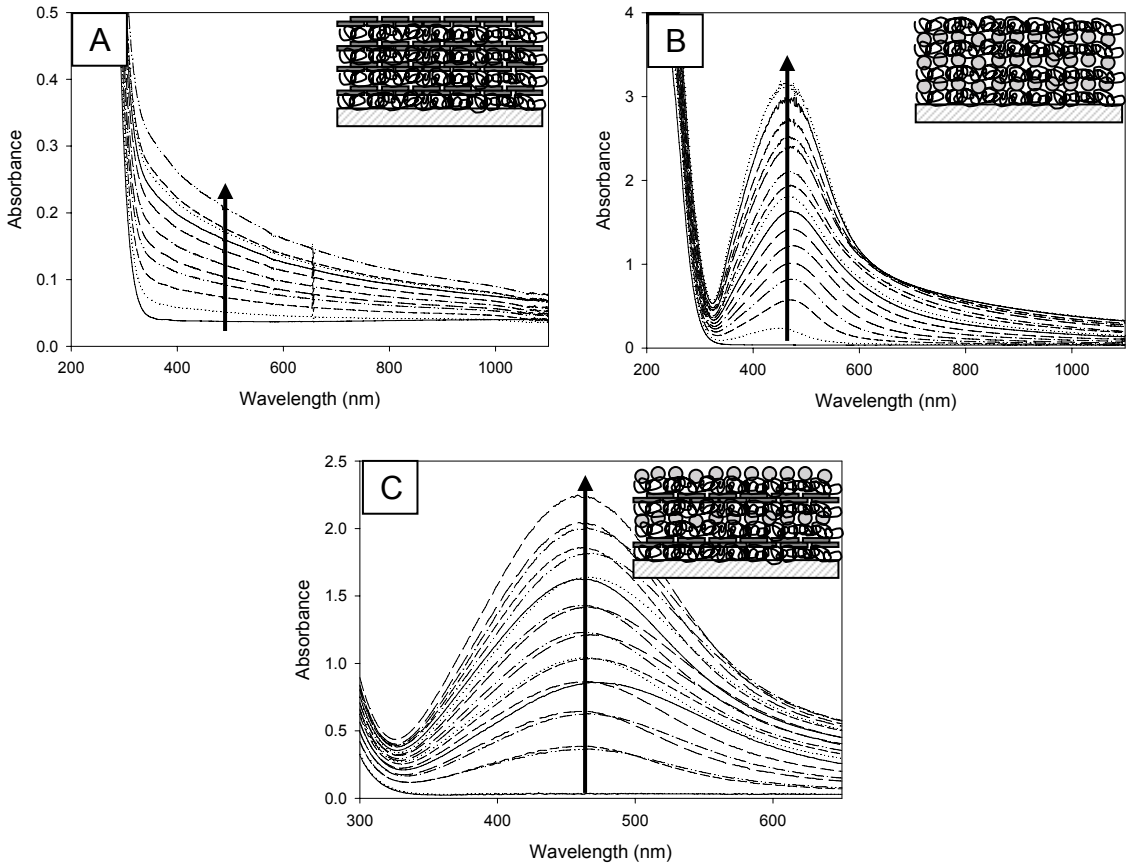


**Figure 3.** UV-vis absorbance spectra of Layer-by-Layer assembly: A - schematic diagram of internal architecture and absorbance spectra for $(PDDA/MTM)_{10}$ assembly; B - schematic diagram of internal architecture and absorbance spectra for $(PDDA/Ag\ NPs)_{15}$ assembly; and C - schematic diagram of internal architecture and absorbance spectra for the hybrid $(PDDA/MTM/PDDA/Ag\ NPs)_{10}$ assembly. Arrows indicate direction of increase in absorbance.

***Assembly of (PDDA/Ag NPs) Composites.***

Prior to assembling the hybrid clay-Ag NPs composite, a PDDA-Ag NPs system (Figure 3B, inset) was first generated in order to establish appropriate assembly conditions. Priming of the glass slides with $(PDDA/PAA)_3$ and 10 minute adsorption steps resulted in successful formation of the multilayer. Similarly to the (PDDA/MTM) system, Figure 3B shows the compilation of the UV-vis absorbance spectra of a (PDDA/Ag NPs) LBL assembly with ten-minute immersions for each layer and with data collected after each (PDDA/Ag NPs) bilayer for up to fifteen bilayers. The height of the Ag absorbance peak increases linearly with each deposited bilayer, suggesting uniform deposition of Ag NPs throughout the film. This observation was also confirmed visually, as the glass slides evenly changed from clear to a deep yellow-brown, metallic color as the number of deposited layers increased. The red shift in plasmon absorption peak maximum from 410 nm to 460 nm should be attributed to dipole resonance interactions between layers of Ag NPs, a well-documented phenomenon in noble metal NPs.[35-41]

***Combined Assembly of MTM and Ag NPs into (PDDA/MTM/PDDA/Ag NPss) Hybrid Composites.***

Having established the optimum assembly parameters for (PDDA/Ag NPs) system, the combined assembly of (PDDA/Ag NPs/PDDA/MTM) films (Figure 3C, inset) was realized in the same fashion, namely: 10 min adsorption steps with glass slides primed with $(PDDA/PAA)_3$. UV-Vis absorbance spectra were again collected after each (PDDA/MTM) and (PDDA/Ag NPs) cycle to verify successful deposition. The compiled data, shown in Figure 3C, display the same incremental increases in absorbance as for the (PDDA/Ag NPs) and (PDDA/MTM) samples. A red-shift in Ag absorbance from 410 nm to 460 nm is again present, and absorbance increases linearly with each deposited layer, indicating proper Ag NPs deposition. The deposition of MTM in each cycle was found to stretch and slightly red-shift the maximum of the peak, from 460 nm to 465-470 nm. Subsequent deposition of (PDDA/Ag NPs) resulted in reversal of the effect to the original value. The slight red shift can be explained by high value of MTM's dielectric constant, $\varepsilon$ = 100-550 [42], as compared to typical values for polyelectrolytes of $\varepsilon \approx 10$. [43] The groups of P. Mulvany and L. M. Liz-Marzan have developed a model for gold NPs LBL film[41], showing that increasing volume fraction of NPs results in red-shift of the peak. At the same time it is expected that increasing separation between Ag NPs layers, will lead to a blue-shift of the spectrum.[41] MTM has been shown to increase overall dielectric constant of a polyelectrolyte composite up to 7 times at volume fractions as low as 5%.[44] In our system, we believe that we are observing a combined effect of the blue-shift from separation increase and red-shift from the MTM inclusion. It can be also expected that subsequent inclusion of the PDDA/Ag NPs layer decreases the volume fraction of MTM which leads to reversal of the effect. Similarly to previous observations, the combined film gradually turned metallic deep-brown with increasing number of layers. Opaqueness was also present with each additional MTM layer added, which was not seen in the (PDDA/Ag NPs) system. This fact is a simple visual criterion for incorporation of MTM layers and successful assembly of the hybrid.

***Bactericidal Properties of the Hybrid Composites.***

Silver has long been known to be a potent antimicrobial agent[45] and its beneficial effects on wound biology have in general been overlooked until recently. Silver ions and silver compounds are known to be potent antimicrobial agents against most of bacteria including *E. coli*,[46-48] while only a few rare strains are silver-resistant.[49-51] In its uncharged state, in the form of Ag NPs, silver was also found to possess antimicrobial properties. Although the mechanism of action is still unresolved, it has been shown that Ag NPs interact with the constituents of the outer membrane, causing structural changes, degradation, and finally cell death.[52] An additional beneficial effect of Ag NPs, which may present an additional advantage for wound healing around implanted material, is anti-inflammatory property.[53] While experiments against bacteria with Ag NPs in solution showed eventual depletion of silver and only growth delay[52], LBL assembly allows for immobilization of Ag NPs in ultra thin films on complicated geometries. Combined with high strength, this coating method offers new alternative for biomedical, implantable devices.

To establish bactericidal properties of our composite, a suspension of bacterial cells (*E. coli*) was placed in a round-bottom test tube together with rectangular piece of a glass slide coated with 10 deposition cycles of the composite. Experiments were carried out both under static and dynamic (shaking) conditions. After 18 hours of incubation the concentration of cells inside the tubes was measured and compared to the inoculation conditions. When the experiments were performed under dynamic conditions, with initial bacteria concentration,

OD600 = 0.0048, almost complete inhibition was observed (Table 1). The supernatant was further plated onto agar plates at 10x dilutions with fresh medium. Both original and diluted suspensions grew into viable colonies overnight with CFU reaching that of control plates. This suggests that the inhibition of bacteria can be attributed to the direct interaction of the cells with the silver immobilized in the composite. The fact that single layer of Ag NPs is much less effective then 10 layers also shows that certain concentration of silver is required for high levels of inhibition at these bacterial concentrations.

**Table 1.** Bacterial inhibition with a hybrid composite under dynamic conditions. Initial optical densities were OD600 = 0.0048 and 0.066. OD 600 measurements of bacterial suspensions were measured after 18 hours of incubation. Comparison was against bare glass slides (Control) and to glass slides coated with $(PDDA/PAA)_3$ (Precoat). Control solutions which reached high OD600 were diluted 30 times before taking the measurement. At least 3 measurements were performed for 3 samples each time and the results are shown as averages of these results.

| Inaculation OD600 | | OD600 |
|---|---|---|
| 0.0048 | Control | 2.002 ± 0.267 |
| | (AgNPs/MTM)10 | 0.0071 ± 0.28 |
| | (AgNPs/MTM)10 + (PDDA/MTM)1 | 0.0047 ± 0.28 |
| 0.066 | Control | 2.096 ± 0.101 |
| | Precoat | 2.492 ± 0.032 |
| | (AgNP's/MTM)1 | 2.477 ± 0.092 |
| | (AgNP's/MTM)10 | 0.193 ± 0.030 |

Further experiments with higher initial concentration of bacteria, OD600 = 0.066, show slightly decreased effectiveness of the composite (Table 1). In analogy to the first result, we found that single layer of silver does not present high enough concentration to provide effective inhibition. We also found that the inhibition can mostly be attributed to the presence of silver and not to any of the poly-ions (PDDA and PAA) or clay.

Under static conditions we have observed very little inhibition, <10 %. The concentration of cells in the control after 18 hours of incubation reached OD600 = 0.949 ± 0.055 whereas for the coated slides the concentration reached OD600 = 0.853 ± 0.023 (initial concentration was OD600 = 0.066). The overall concentration of cells was lower as compared to the agitated experiments, but this can be attributed to decreased diffusion of oxygen and thus starvation. After 18 hours, cells have settled into the meniscus below the glass slide hence avoiding contact with the composite. The growth process was most likely retarded during sedimentation were small percentage of the cells came in contact with the surface.

***Silver Elution from the Hybrid Composite.***

Antimicrobial properties of these composites are attributed to the Ag NPs immobilized on the surface of this material. Hence, evaluation of the stability of the composite in aqueous medium is important for long term durability and effectiveness. None of the previous studies have attempted determination of the actual amount of silver eluting from such composites. This is important because high concentration of oxidized silver, $Ag^+$, can be toxic for human cells[54-56] and potentially cause adverse effects for long-term implants. Considering high surface energy and therefore greater chemical potential of silver in NPs, the actual amount of silver could be substantially higher than for bulk pieces of the same metal. In order to determine

actual amounts of eluted silver, glass slides coated with $(PDDA/MTM/PDDA/Ag\ NPs)_{10}$ were immersed in de-ionized water for 25 days, with solution aliquots collected at regular intervals and analyzed by ICP-MS for trace levels of Ag leaching out from the composite. Samples were collected from slides placed in both light and dark conditions in order to account for possible Ag NPs photoreactivity. After 25 days, films retained their integrity and no visible change in water color was observed in either light or dark environments. ICP-MS analysis of the sample aliquots retained after different time intervals showed that silver was eluting in miniscule concentrations in the range of 0.5-2.0 and 0-3.3 μg/L for dark and light conditions correspondingly (Figure 4). Therefore, one can say that the overall silver concentration around the implanted LBL nanocomposite $(PDDA/MTM/PDDA/Ag\ NPs)_{10}$ does not exceed 3.0 μg/L.

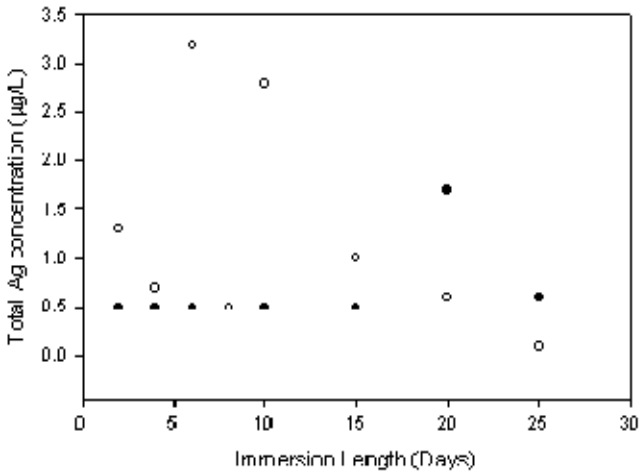


**Figure 4.** Analysis of the hybrid MTM-Ag NPs' composite film stability for Ag elution. ICP-MS analysis of the water solution after immersion shows levels of Ag below the detection limit of the instrument. Both Dark (filled symbol) and Light (open symbol) conditions show similar results.

***Biocompatibility Evaluation.***

Although the concentration of eluting silver is very small, direct evaluation of the biocompatibility of the composite would be necessary for further studies of this material. Ag NPs have been shown to possess good biocompatibility with mouse fibroblasts and human osteoblasts[57] and their use for bio-applications has been widely documented.[58-60] To evaluate the effect of our composite, glass slides coated with the films were cut into smaller pieces and placed in the 12-well plates. Following sterilization with 70% EtOH and UV-vis irradiation, cells were seeded on top of the slides and allowed to attach and grow for 3 days. One of the indications of biocompatibility characteristics of this cell line is their attachment to the surface. Figure 5 shows cells attaching on the surface of the composite. The number of attaching cells was not as high as for the bare slides however it is possible to render the composite more biocompatible by coating with additional components. When additional capping layers were introduced on top of the composite, no change in antibacterial properties was observed (Table 1). The same experiment was repeated with 5 bilayers of (PDDA/MTM) of capping (data not shown) and the same level of inhibition was achieved. This suggests that additional, interfacing layers could be introduced on top of the composite to improve the cell attachment without having to sacrifice the bactericidal properties.

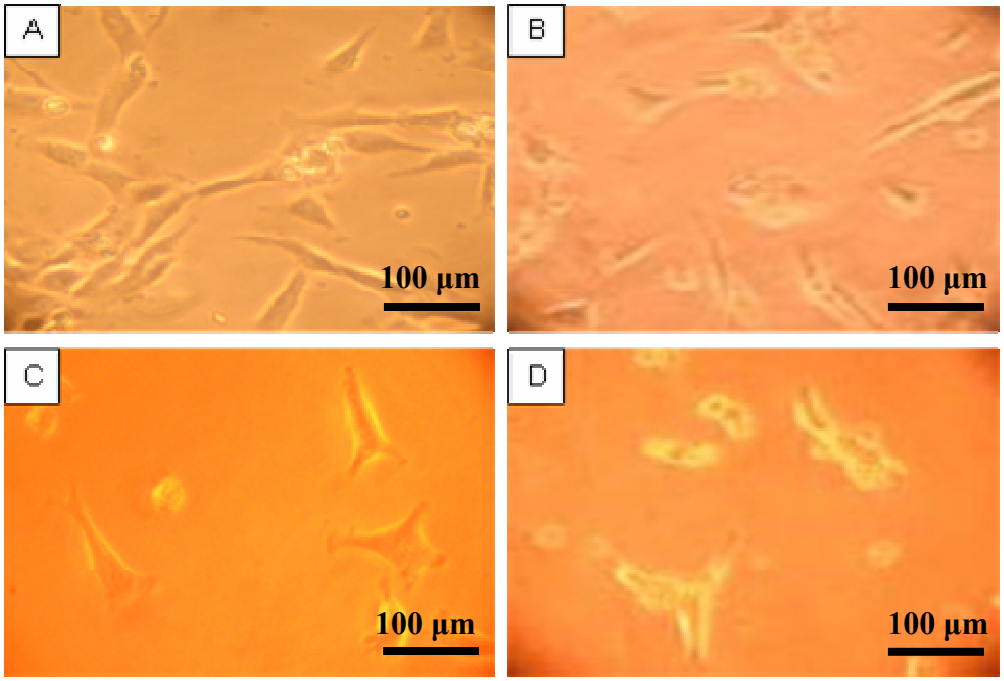


**Figure 5.** Optical microscopy images of Human Osteoblasts (ATCC, CRL-11372) cultured on bare glass slides (A and B) and on glass slides coated with $(PDDA/MTM/PDDA/Ag\ NPs)_{10}$ (C and D) for 3 days.

## CONCLUSIONS

We have presented here preparation of a nanostructured, hybrid and multifunctional, composite containing Ag NPs with good mechanical properties. The composite possesses strong antibacterial characteristics as well as biocompatibility with human osteoblasts. With wide variety of materials available, this type of composites can be expanded to additional functionalities.

## ACKNOWLEDGMENTS

The authors thank Ciba-Vision, NSF-BioPhotonics, AFOSR and DARPA for support of this research. PP thanks Bong-Sup Shim at the UofM Department of Chemical Engineering for useful suggestions with layer-by-layer assembly process.

## REFERENCE LIST

1. Lvov, Y.; Essler, F.; Decher, G. *J. Phys. Chem.* **1993**; *97*, 13773.
2. Mamedov, A.; Belov, A.; Giersig, M.; Mamedova, N.; Kotov, N. *J. Amer. Chem. Soc.*, **2001**, *123*, 7738.
3. Wang, D.; Rogach, A.; Caruso, F. *Nano Letters* **2002**, *2*, 857.
4. Liu, J.; Cheng, L.; Song, Y.; Liu, B.; Dong, S. *Langmuir* **2001**, *17*, 6747.
5. Shen, Y.; Liu, J.; Jiang, J., Liu B.; Dong, S. *J. Phys. Chem. B* **2003**, *107*, 9744.
6. Wang, Y.; Wang, X.; Guo, Y.; Cui, Z.; Lin, Q.; Yu, W.; Liu, L., Xu, L.; Zhang, D.; Yang, B. *Langmuir* **2004**, *20*, 8952.
7. Salgueiriño-Maceira, V.; Caruso, F.; Liz-Marzán, L. *J. Phys. Chem. B* **2003**, *107*, 10990.
8. Nolte, A.; Rubner, M.; Cohen, R. *Langmuir* **2004**, *20*, 3304.
9. Mamedov, A.; Ostrander, J.; Aliev, F.; Kotov, N. *Langmuir* **2000**, *16*, 3941.

10. Aliev, F.; Correa-Duarte, M.; Mamedov, A.; Ostrander, J.; Giersig, M.; Liz-Marzán, L.; Kotov, N. *Adv. Mat.* **1999**, *11*, 1006.
11. Constantine, C.; Gattás-Asfura, K.; Mello, S.; Crespo, G.; Rastogi, V.; Cheng, T.; DeFrank, J.; Leblanc, R. *Langmuir* **2003**, *19*, 9863.
12. Constantine, C.; Gattás-Asfura, K.; Mello, S.; Crespo, G.; Rastogi, V.; Cheng, T.; DeFrank, J.; Leblanc, R.; *J. Phys. Chem. B* **2003**, *107*, 13762.
13. Zheng, H.; Rubner, M.; Hammond, P. *Langmuir* **2002**, *18*, 4505.
14. Jukes, P.; Heriot, S.; Sharp, J.; Jones, R. *Macromol.* **2005**, *38*, 2030.
15. Crisp, M.; Kotov, N. *Nano Letters* **2003**, *3*, 173.
16. Mamedov, A.; Kotov, N.; *Langmuir* **2000**, *16*, 5530.
17. Sinani, V; Koktysh, D.; Yun, B.; Matts, R.; Pappas, T.; Motamedi, M.; Thomas, S.; Kotov, N. *Nano Letters* **2003**, *3*, 1177.
18. Malikova, N.; Pastoriza-Santos, I.; Schierhorn, M.; Kotov, N.; Liz-Marzán, L. *Langmuir* **2002**, *18*, 3694.
19. Tang, Z.; Kotov, N.; Magonov, S.; Ozturk, B. *Nature Materials* **2003**, *2*, 413.
20. Jiang, C.; Markutsya, S.; Pikus, Y.; Tsukruk, V. V. *Nature Materials* **2004**, 3, 721.
21. Jiang, C.; Markutsya, S.; Tsukruk, V. V. *Advanced Materials*, **2004**, *16*, 157.
22. Yang, S.; Lee, D.; Cohen, R.; Rubner, M. F. *Langmuir* **2004**, *20*, 5978.
23. Yang, S. Y.; Berg, M. C.; Hammond, P. T.; Rubner, M. F. *Polymeric Materials Science and Engineering* **2003**, *89*, 79.
24. Richert, L.; Boulmedais, F.; Lavalle, P.; Mutterer, J.; Ferreux, E.; Decher, G.; Schaaf, P.; Voegel, J.-C.; Picart, C. *Biomacromolecules* **2004**, *5*, 284.
25. Kidambi, S.; Lee, I.; Chan, C. *Polymer Preprints* **2004**, *45*, 88.
26. Zhu, Y.; Gao, C.; He, T.; Liu, X.; Shen, J. *Biomacromol.* **2003**, *4*, 446.
27. Bhadra, D.; Gupta, G.; Bhadra, S.; Umamaheshwari, R. B.; Jain, N. K. *Journal of Pharmacy & Pharmaceutical Sciences* **2004**, *7(2)*, 241.
28. Boulmedais, F.; Frisch, B.; Etienne, O.; Lavalle, Ph.; Picart, C.; Ogier, J.; Voegel, J.-C.; Schaaf, P.; Egles, C. *Biomaterials*, **2004**, *25*, 2003.
29. Kenausis, G. L.; Voros, J.; Elbert, D. L.; Huang, N.; Hofer, R.; Ruiz-Taylor, L.; Textor, M.; Hubbell, J. A.; Spencer, N. D. *Journal of Physical Chemistry B*, **2000**, *104*, 3298.
30. Etienne, O.; Picart, C.; Taddei, C.; Haikel, Y.; Dimarcq, J. L.; Schaaf, P.; Voegel, J. C.; Ogier, J. A.; Egles, C. *Antimicrobial Agents and Chemotherapy,* **2004**, *48(10)*, 3662.
31. Dai, J.; Bruening, M. *Nano Letters* **2002**, *2*, 497.
32. Shi, Z.; Neoh, K. G.; Kang, E. T. *Langmuir* **2004**, *20*, 6847.
33. Balogh, L.; Swanson, D.; Tomalia, D.; Hagnauer, G.; McManus, A. *Nano Letters* **2001**, *1*, 18
34. Raveendran, P.; Fu, J.; Wallen, S. *J. Amer. Chem. Soc.* **2003**, *125*, 13940.
35. Zhao, L.; Kelly, K.; Schatz, G. *J. Phys. Chem.* **2003**, *107*, 7343.
36. Jensen, T.; Kelly, L.; Lazarides, A.; Schatz, G. *J. Clus. Sci.* **1999**, *10*, 295.
37. Kobayashi, Y.; Katakami, H.; Mine, E.; Nagao, D.; Konno, M.; Liz-Marzan, L. M. *Journal of colloid and interface science* **2005**, *283*, 392.
38. Liz-Marzan, L. M.; Lado-Tourino, I. *Langmuir* **1996**, *12*, 3585.
39. Pastoriza-Santos, I.; Liz-Marzan, L. M. *Langmuir* **1999**, *15*, 948.
40. Pastoriza-Santos, I.; Gomez, D.; Perez-Juste, J.; Liz-Marzan, L. M.; Mulvaney, P. *Physical Chemistry Chemical Physics* **2004**, *6*, 5056.
41. Ung, T.; Liz-Marzan, L. M.; Mulvaney, P. *Colloids and Surfaces, A: Physicochemical and Engineering Aspects* **2002**, *202*, 119.

42. Arroyo, F. J.; Carrique, F.; Jimenez-Olivares, M. L.; Delgado, A. V. *Journal of Colloid and Interface Science* **2000**, *229*, 118.
43. Anderson, M. R.; Davis, R. M.; Taylor, C. D.; Parker, M.; Clark, S.; Marciu, D.; Miller, M. *Langmuir* **2001**, *17*, 8380.
44. Lu, J.; Zhao, X. *International Journal of Modern Physics B: Condensed Matter Physics*, *Statistical Physics, Applied Physics* **2002**, *16*, 2521.
45. Goodman & Gilman's the pharmacological basis of therapeutics., 10th ed. / edited by Hardman, J. G. and Limbird, L. E., New York: McGraw-Hill Medical Pub. Division, c2001.
46. Slawson, R. M.; Van Dyke, M. I.; Lee, H.; Trevors, J. T. *Plasmid*, **1992**, *27*, 72.
47. Zhao, G. J.; Stevens, S. E. *Biometals*, **1998**, *11*, 27.
48. Spadro, J. A.; Berger, T. J.; Barranco, S. D.; Chapin, S. E.; Becker, R. O. *Microb. Agents Chemother.*, **1974**, *6*, 637.
49. Pooley, F. D. *Nature*, **1982**, *296*, 642.
50. Slawson, R. M.; Trevors, J. T.; Lee, H.; *Arch. Microbiol.*, **1992**, *158*, 398.
51. Klaus, T.; Joerger, R.; Olsson, E.; Granqvist, C.-G. *Proc. Natl. Acad. Sci. U.S.A.*, **1999**, *96*, 13,611.
52. Sondi, I., Salopek-Sondi, B. *Journal of Colloid and Interface Science*, **2004**, *275*, 177.
53. Bhol, K. C.; Schechter, P. J., *British Journal of Dermatology*, **2005**, *152(6)*, 1235.
54. Locci, P.; Marinucci, L.; Lilli, C.; Belcastro, S.; Staffolani, N.; Bellocchio, S.; Damiani, F.; Becchetti, E. *Journal of Biomedical Materials Research* **2000**, *51*, 561.
55. Wataha, J. C.; Lockwood, P. E.; Schedle, A. *Journal of Biomedical Materials Research* **2000**, *52*, 360.
56. Cortizo, M. C.; De Mele, M. F. L.; Cortizo, A. M. *Biological Trace Element Research* **2004**, *100*, 151.
57. Alt, V.; Bechert, T.; Steinrucke, P.; Wagener, M.; Seidel, P.; Dingeldein, E.; Domann, E.; Schnettler, R. *Biomaterials*, **2004**, *25*, 4383.
58. Vo-Dinh, T.; Yan, F.; Wabuyele, M. B. *Journal of Raman Spectroscopy*, **2005**, *36(6/7)*, 640.
59. Ren, C.; Song, Y.; Li, Z.; Zhu, G. *Analytical and Bioanalytical Chemistry* **2005**, *381(6)*, 1179.
60. Xu, X.-H. N.; Patel, R. N. *Encyclopedia of Nanoscience and Nanotechnology*, **2004**, *7*, 181.